ELSEVIER

Thermochimica Acta 293 (1997) 153–161

thermochimica acta

Thermal study of areneruthenium(II) derivatives

Gregorio Sánchez[a], Joaquín García[a], José Pérez[a], Gabriel García[a], Gregorio López[a,*], Gloria Víllora[b]

[a]*Departamento de Química Inorgánica, Campus Universitario de Espinardo, Universidad de Murcia, Apto Correos 4021, 30071 Murcia, Spain*

[b]*Departamento de Ingeniería Química, Universidad de Murcia, 30071 Murcia, Spain*

Received 15 February 1996; accepted 12 December 1996

Abstract

The TG and DTG study of areneruthenium(II) derivatives [Ru(arene)Cl_2L] (arene = benzene or *p*-cymene (*p*-$MeC_6H_4CHMe_2$); *L* = aniline, diethylamine, dimethylsulfoxide, tetrahydrothiofene or dimethylsulfide) was carried out under a dynamic air atmosphere. The kinetics of the first step of thermal decomposition were evaluated from the dynamic weight loss data by means of Coats–Redfern, MacCallum–Tanner and Horowitz–Metzger methods. The D_n and R_n models were selected as the models best fitting the experimental TG curves. The values of activation energy, *E*, and frequency factor, *A*, of the thermal decomposition were calculated. © 1997 Elsevier Science B.V.

Keywords: Ruthenium; η^6-Arene complexes; Thermal behaviour

1. Introduction

The reaction of [{Ru(η^6-arene)Cl(μ-Cl)}$_2$] (arene = benzene, *p*-cymene) towards neutral mono- and bidentate ligands have been widely studied and recently reviewed [1]. Cleavage of the chloride bridges gives monomeric complexes [Ru(η^6-arene)Cl_2L] [2,3] and a simple method of regenerating areneruthenium dichloride dimers from their monomeric adducts has been reported [4].

Here we describe the thermal behaviour of ruthenium complexes of the type [Ru(η^6-arene)Cl_2L] [arene = benzene, *p*-cymene; *L* = aniline ($PhNH_2$), diethylamine (Et_2NH), dimethylsulfoxide (DMSO), tetrahydrothiophene (THT), and dimethylthioether (Me_2S)] and determination of the kinetics and the values of activation energy, *E*, and frequency factor, *A*, of the thermal decomposition were calculated by means of Coats–Redfern, MacCallum–Tanner and Horowitz–Metzger methods. A similar study on pentamethylcyclopentadienyl rhodium (III) derivatives has been reported [5].

2. Experimental

2.1. Preparation of complexes

The complexes [{Ru(η^6-arene)Cl(μ-Cl)}$_2$] were prepared by published methods [6,7] and the neutral ligands were commercial grade chemicals. The solvents were dried by conventional methods.

*Corresponding author.

PII S0040-6031(97)00007-5

The complexes [Ru(η^6-arene)Cl_2L] were obtained by reaction of the dinuclear complexes [{Ru(η^6-arene)Cl(μ-Cl)}$_2$] with the corresponding neutral ligands in CH_2Cl_2 solution according to the following general method [8]. The neutral ligand ($PhNH_2$, Et_2NH, DMSO, THT or Me_2S respectively; 0.32 mmol) in dichloromethane (5 ml) was added to a solution of [{Ru(η^6-arene)Cl(μ-Cl)}$_2$] (0.16 mmol) in dichloromethane (10 ml). After 1 h of constant stirring, the resulting red solution was concentrated under reduced pressure; the addition of diethyl ether caused the formation of complexes, which were filtered off and air-dried.

The isolated complexes gave satisfactory partial elemental analyses and were characterized by spectroscopic methods. The relevant data are given below.

2.2. Characterization

The C, H, N and S analyses were performed with a Carlo Erba microanalyser. IR spectra were recorded on a Perkin–Elmer 16F PC FT-IR spectrophotometer using Nujol mulls between polyethylene sheets and ^1H and ^{13}C NMR spectra on a Brucker AC 200E or a Varian 300 instrument.

[Ru(η^6-benzene)$Cl_2(PhNH_2)$] (**1a**). Orange crystals, yield 84%. Analysis: found (%): C, 42.1; H, 4.0; N, 4.2; calc.: C, 41.0; H, 3.8; N, 4.1. ν(Ru–Cl) 264 cm^{-1}. ^1H NMR (DMSO-d_6), δ: 6.98 (m, 2H, Ph), 6.51 (m, 3H, Ph), 5.96 (s, 6H, benzene), 4.99 (s, br, 2H, NH_2). ^{13}C NMR (DMSO-d_6), δ: 148.7 (Ph), 128.9 (Ph), 115.7 (Ph), 114.0 (Ph), 87.8 (benzene).

[Ru(η^6-*p*-cymene)$Cl_2(PhNH_2)$] (**1b**). Orange crystals, yield 68%. Analysis: found (%): C, 48.2; H, 5.5; N, 3.3; calc.: C, 48.1; H, 5.3; N, 3.5. ν(Ru–Cl) 276 cm^{-1}. ^1H NMR (DMSO-d_6), δ: 6.98 (m, 2H, Ph), 6.50 (m, 3H, Ph), 5.77 (m, 4H, *p*-cymene), 4.97 (s, br, 2H, NH_2), 2.81 (sp, 1H, C*H*Me_2), 2.1 (s, 3H, CH_3-*p*), 1.2 (d, 6H, CH*Me*$_2$). ^{13}C NMR (DMSO-d_6), δ: 148.5 (Ph), 128.9 (Ph), 115.8 (Ph), 114.0 (Ph), 106.5 (C-^{i}Pr), 100.2 (C-Me), 86.4 (C_{ring}), 85.6 (C_{ring}), 30.1 (*C*H-Me_2), 21.6 (CH-*Me*$_2$), 18.0 (Me).

[Ru(η^6-benzene)$Cl_2(Et_2NH)$] (**IIa**). Orange crystals, yield 72%. Analysis: found (%): C, 37.4; H, 5.4; N, 4.2; calc.: C, 37.2; H, 5.3; N, 4.3. ν(Ru–Cl) 268 cm^{-1}. ^1H NMR ($CDCl_3$), δ: 5.6 (s, 6H, benzene), 3.3 (q, 4H, Et), 2.45 (s, br, 1H, NH), 1.20 (t, 6H, Et), 4.99. ^{13}C NMR (DMSO-d_6), δ: 82.9 (benzene), 51.2 (Et), 15.6 (Et).

[Ru(η^6-*p*-cymene)$Cl_2(Et_2NH)$] (**IIb**). Orange crystals, yield 76%. Analysis: found (%): C, 44.2; H, 6.5; N, 3.4; calc.: C, 44.3; H, 6.6; N, 3.7. ν(Ru–Cl) 248 cm^{-1}. ^1H NMR(DMSO-d_6), δ: 5.8 (m, 4H, *p*-cymene), 2.8 (sp, 1H, C*H*Me_2), 2.5 (q, 4H, Et), 2.1 (s, 3H, CH_3-*p*), 1.2 (d, 6H, CH*Me*$_2$), 1.0 (t, 6H, Et). ^{13}C NMR (DMSO-d_6), δ: 106.5 (C-^{i}Pr), 100.2 (C-Me), 86.5 (C_{ring}), 85.6 (C_{ring}), 43.2 (Et), 30.1 (*C*H-Me_2), 21.6 (CH-*Me*$_2$), 18.0 (Me), 14.6 (Et).

[Ru (η^6-benzene)Cl_2(DMSO)] (**IIIa**). Orange crystals, yield 84%. Analysis: found (%): C, 29.4; H, 3.4; S, 9.5; calc.: C, 29.3; H, 3.7; S, 9.8. ν(Ru–Cl) 280 cm^{-1}. ^1H NMR (DMSO-d_6), δ: 6.0 (s, 6H, benzene), 2.5 (s, 6H, DMSO). ^{13}C NMR (DMSO-d_6), δ: 87.7 (benzene), 40.5 (DMSO).

[Ru(η^6-*p*-cymene)Cl_2(DMSO)] (**IIIb**). Orange crystals, yield 82%. Analysis: found (%): C, 37.8; H, 5.4; S, 8.4; calc.: C, 37.5; H, 5.2; S, 8.3. ν(Ru–Cl) 260 cm^{-1}. ^1H NMR(DMSO-d_6), δ: 5.8 (m, 4H, *p*-cymene), 2.8 (sp, 1H, C*H*Me_2), 2.5 (q, 6H, DMSO), 2.1 (s, 3H, CH_3-*p*), 1.2 (d, 6H, CH*Me*$_2$). ^{13}C NMR (DMSO-d_6), δ: 106.5 (C-^{i}Pr), 100.2 (C-Me), 86.5 (C_{ring}), 85.6 (C_{ring}), 40.5 (DMSO), 30.1 (*C*H-Me_2), 21.6 (CH-*Me*$_2$), 18.0 (Me).

[Ru(η^6-benzene)Cl_2(THT)] (**IVa**). Orange crystals, yield 78%. Analysis: found (%): C, 35.4; H, 4.4; S, 9.7; calc.: C, 35.5; H, 4.2; S, 9.5. ν(Ru–Cl) 268 cm^{-1}. 1H NMR (DMSO-d_6), δ: 6.0 (s, 6H, benzene), 2.7 (t, 4H, THT), 1.8 (t, 4H, THT). ^{13}C NMR (DMSO-d_6), δ: 87.7 (benzene), 31.2 (THT), 30.8 (THT).

[Ru(η^6-*p*-cymene)Cl_2(THT)] (**IVb**). Orange crystals, yield 76%. Analysis: found (%): C, 42.8; H, 5.4; S, 8.4; calc.: C, 42.6; H, 5.6; S, 8.1. ν(Ru–Cl) 286 cm^{-1}. ^1H NMR(DMSO-d_6), δ: 5.8 (m, 4H, *p*-cymene), 2.8 (sp, 1H, C*H*Me_2), 2.7 (t, 4H, THT), 2.1 (s, 3H, CH_3-*p*), 1.8 (t, 4H, THT) 1.2 (d, 6H, CH*Me*$_2$). 13C NMR (DMSO-d_6), δ: 106.4 (C-^{i}Pr), 100.2 (C-Me), 86.6 (C_{ring}), 85.6 (C_{ring}), 31.2 (THT), 30.1 (*C*H-Me_2), 21.6 (CH-*Me*$_2$), 18.0 (Me).

[Ru(η^6-benzene)$Cl_2(Me_2S)$] (**Va**). Orange crystals, yield 78%. Analysis: found (%): C, 30.6; H, 3.5; S, 10.5; calc.: C, 30.8; H, 3.9; S, 10.3. ν(Ru–Cl) 272 cm^{-1}. ^1H NMR (DMSO-d_6), δ: 6.0 (s, 6H, benzene), 2.0 (s, 6H, Me_2S). ^{13}C NMR (DMSO-d_6), δ: 87.7 (benzene), 17.4 (Me_2S).

[Ru(η^6-*p*-cymene)$Cl_2(Me_2S)$] (**Vb**). Orange crystals, yield 72%. Analysis: found (%): C, 39.3; H, 5.7; S, 8.9; calc.: C, 39.1; H, 5.5; S, 8.7. ν(Ru–Cl) 288 cm^{-1}. ^1H NMR, δ: (DMSO-d_6) 5.8 (m, 4H, *p*-cymene), 2.8 (sp, 1H, C*H*Me_2), 2.1 (s, 3H, CH_3-*p*), 2.0 (s, 6H, Me_2S), 1.2 (d, 6H, CH*Me*$_2$). ^{13}C NMR (DMSO-d_6), δ: 106.5 (C-^{i}Pr), 100.2 (C-Me), 86.6 (C_{ring}), 85.6 (C_{ring}), 30.1 (*C*H-Me_2), 21.6 (CH-*Me*$_2$), 18.0 (Me), 17.4 (Me_2S).

2.3. Thermal analysis

Thermoanalytical data were obtained from TG and DTG curves. These were recorded on a Metter TA-3000 system provided with a Metter TG-50 thermobalance. The atmosphere used was an air flow (50 ml min^{-1}). The heating rate was 5°C min^{-1} with samples of less than 10 mg.

3. Results and discussion

3.1. Thermal stability

Table 1 list the steps, initial and final temperatures, partial and total mass losses and maximum peak for each step in the thermal decomposition of the complexes.

The TG–DTG curves for the compounds in the air atmosphere are shown in Figs. 1 and 2. All the complexes decompose on heating to give the binuclear runtheniumarene complex [{Ru(η^6-arene)Cl(μ-Cl)}$_2$], according to Eq. (1).

$$[Ru(\eta^6\text{-arene})Cl_2L] \rightarrow \tfrac{1}{2}[Ru(\eta^6\text{-arene})Cl(\mu\text{-}Cl)]_2 + L$$

The complex [Ru(η^6-benzene)$Cl_2(PhNH_2)$] (**Ia**) loses one aniline molecule between 151 and 214°C (DTG peak, 203°C), to give the dinuclear complex [{Ru(η^6-benzene)Cl(μ-Cl)}$_2$] which decomposes slowly and irregularly between 214 and 372°C to finally give Ru_2O_3. The corresponding *p*-cymene complex (**Ib**) shows a first decomposition stage at a lower temperature than **Ia** (114–198) and the binuclear intermediate chloro complex shows a second step between 198 and 228°C, corresponding to 3/4 mol of Cl_2, to yield a non-isolable intermediate of formula [Ru(η^6-*p*-cymene)]$_2$Cl (13.1% against the theoretical value of 13.3%) which decomposes slowly at 243°C to give Ru_2O_3.

The diethylamine complexes **IIa** and **IIb** are less stable than the aniline complexes and decompose at 116 and 80°C, respectively, to give the chloro-bridged complex.

The complexes [Ru(η^6-benzene)Cl_2L] (L = DMSO, THT and Me_2S) (**IIIa–Va**) are stable up to 122, 110 and 94°C to give the dinuclear chloro-bridged complex, which decomposes at a lower temperature (DTG peaks: 244, 245 and 234°C, respectively) than **Ia** and **IIa**; however, the dinuclear intermediate complex resulting from the decomposition of the *p*-cymene complexes **IIIb–Vb** decompose at temperatures similar to those of **Ib** and **IIb**.

The intermediate chloro-bridged complex can be isolated in every case and identified by IR and ^1H-NMR spectroscopy [8,9]. Ruthenium oxide was obtained as a residue from the decomposition of all the complexes (Table 1).

3.2. Determination of kinetic parameters

Kinetic parameters for the first step of the processes studied in the preceding paragraph were calculated from the TG curves using the Coats–Redfern (CR), MacCallum–Tanner (MT) and Horowitz–Metzger (HM) methods. The following equations were used.

1. The Coats–Redfern equation [10]:

$$\ln\left[\frac{g(\alpha)}{T^2}\right] = \ln\left[\frac{AR}{\beta E}\left(1 - \frac{2RT}{E}\right)\right] - \frac{E}{RT}$$

2. The MacCallum–Tanner equation [11]:

$$\log g(\alpha) = \log\left[\frac{AE}{\beta R}\right] - 0.485E^{0.435} - \frac{[(0.449 + 0.217E) \times 10^3]}{T}$$

3. The Horowitz–Metzger equation [12]:

$$\ln g(\alpha) = \ln\left[\frac{AET_s^2}{\beta E}\right] - \frac{E}{RT_s} + \frac{E\theta}{RT_s^2}$$

Table 1
TG and DTG data for the neutral ruthenium complexes (under dynamic air atmosphere; heating rate 5°C min^{-1})

Complex	Step	Temperature range (°C)	DTG_{max} (°C)	Weight loss(%), found (calc.)	Assignment
Ia	1	151–214	203	26.9 (27.1)	$PhNH_2$
	2	214–372	262	34.8 (36.5)	
	residue	>500	—	36.6 (36.4)	1/2 Ru_2O_3
Ib	1	114–198	172	22.8 (23.3)	$PhNH_2$
	2	198–228	219	13.1 (13.3)	3/4 Cl_2
	3	243–358	261	31.2 (32.0)	
	residue	>500	—	31.4 (31.3)	1/2 Ru_2O_3
IIa	1	116–191	167	22.7 (22.6)	Et_2NH
	2	191–271	261	36.1 (38.7)	
	residue	>500	—	39.8 (38.7)	1/2 Ru_2O_3
IIb	1	80–145	136	19.5 (19.3)	Et_2NH
	2	170–221	209	13.3 (14.0)	3/4 Cl_2
	3	235–342	269	31.0 (33.7)	
	residue	>500	—	33.6 (33.0)	1/2 Ru_2O_3
IIIa	1	122–203	186	21.7 (23.8)	DMSO
	2	203–460	244	37.1 (38.1)	
	residue	>500	—	39.9 (38.1)	1/2 Ru_2O_3
IIIb	1	103–180	154	20.2 (20.3)	DMSO
	2	180–225	213	13.6 (13.9)	3/4 Cl_2
	3	233–346	279	32.1 (33.3)	
	residue	>500	—	31.9 (32.6)	1/2 Ru_2O_3
IVa	1	110–179	168	25.9 (26.0)	THT
	2	211–389	245	33.7 (37.0)	
	residue	>500	—	37.2 (37.0)	1/2 Ru_2O_3
IVb	1	116–179	158	21.8 (22.3)	THT
	2	194–229	213	13.8 (13.5)	3/4 Cl_2
	3	249–375	261	27.9 (32.4)	
	residue	>500	—	32.8 (31.7)	1/2 Ru_2O_3
Va	1	94–181	165	20.0 (19.9)	Me_2S
	2	193–415	234	36.2 (40.0)	
	residue	>500	—	41.5 (40.1)	1/2 Ru_2O_3
Vb	1	63–162	140	17.0 (16.8)	Me_2S
	2	183–226	214	14.6 (14.5)	3/4 Cl_2
	3	247–355	262	32.2 (34.7)	
	residue	>500	—	34.5 (34.0)	

where α is the fraction of the sample decomposed at time t, $\theta = T - T_s$, T_s being the DTG peak temperature, β the heating rate, E the energy of activation, and A the pre-exponential factor. The algebraic expression of integral $g(\alpha)$ functions for the most common mechanism operating in solid-state decompositions

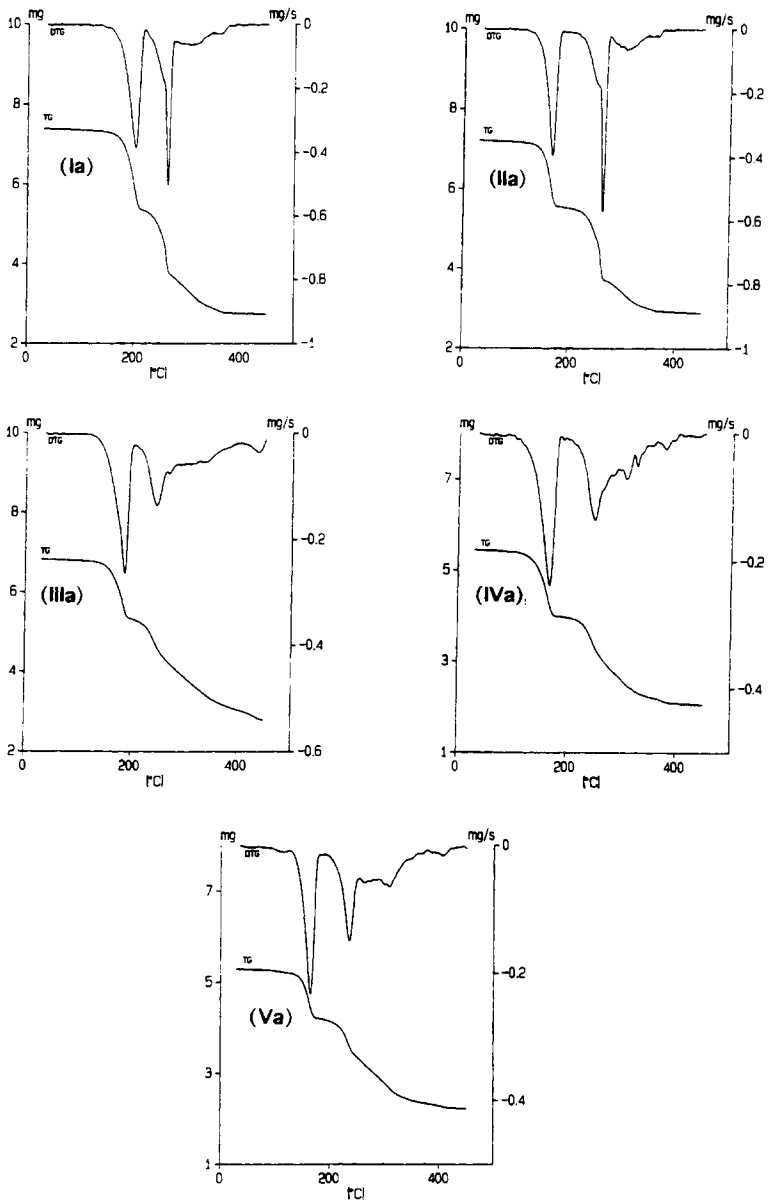

Fig. 1. TG and DTG curves of the η^6-benzene complexes **Ia–Va**.

tested in the present work are listed in Table 2. The kinetic parameters were calculated from the linear plots of the left-hand side of the kinetic equations against $1/T$ for Coats–Redfern and MacCallum–Tanner equations, and for Horowitz–Metzger equation the left-hand side is plotted against θ. The values of E and A were calculated, respectively, from the slope and intercept of the straight lines.

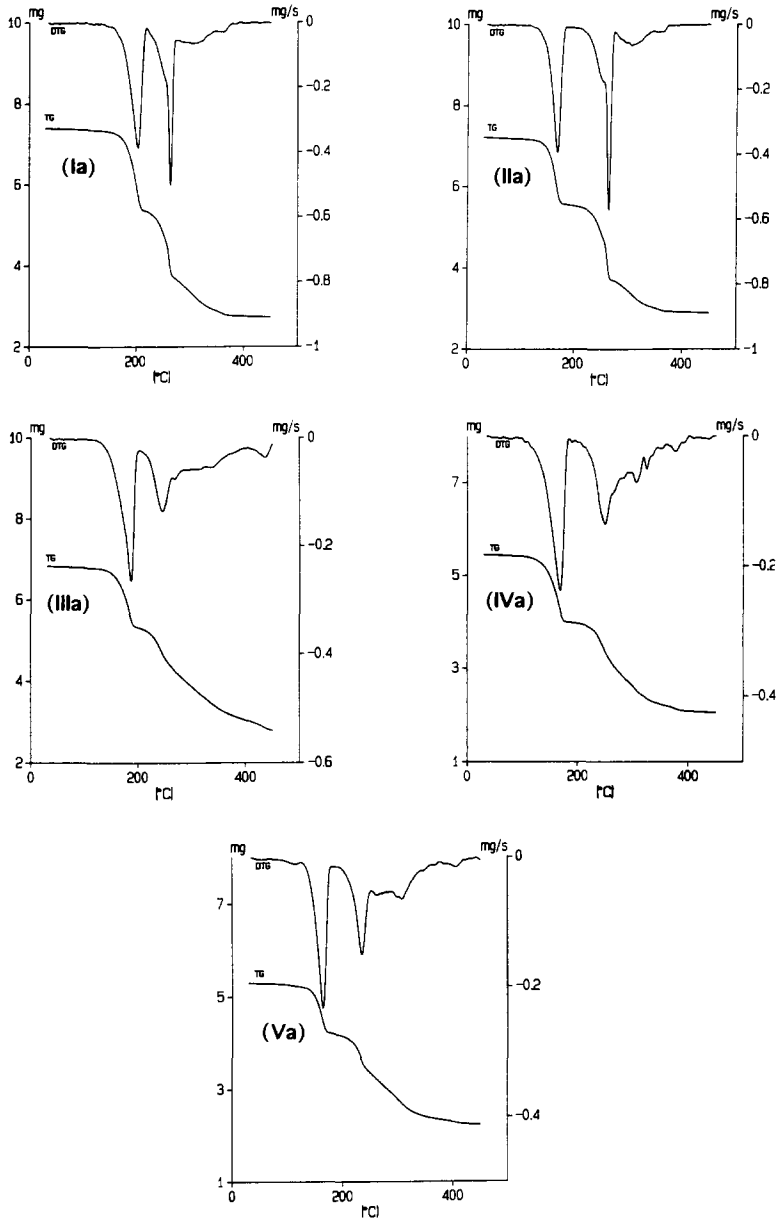

Fig. 2. TG and DTG curves of the η^6-*p*-cymene complexes **Ib–Vb**.

4. Conclusions

Values of the kinetic parameters and linear regression coefficients are listed in Table 3. One should note that there is a good concordance between the results obtained for the mechanism and activation energy of the first step of decomposition of the complexes in Coats–Redfern and MacCallum–Tanner methods. However, the values of the linear regression coefficients do not allow to identify unambiguously the mechanism of the thermal decomposition of the complexes.

Table 2
Rate laws used to analyse kinetic data

Symbol	g(α)	Symbol	g(α)
P3	$\alpha^{1/2}$	A1.5	$[-\ln(1-\alpha)]^{2/3}$
D1	α^2	A2	$[-\ln(1-\alpha)]^{1/2}$
D2	$(1-\alpha)\ln(1-\alpha)+\alpha$	A3	$[-\ln(1-\alpha)]^{1/3}$
D3	$[1-(1-\alpha)^{1/3}]^2$	A4	$[-\ln(1-\alpha)]^{1/4}$
D4	$[1-(2\alpha/3)]-(1-\alpha)^{2/3}$	R1	$1-(1-\alpha)^{2/3}$
F1	$-\ln(1-\alpha)$	R2	$1-(1-\alpha)^{1/2}$
F2	$1/(1-\alpha)$	R3	$1-(1-\alpha)^{1/3}$
F3	$[1/(1-\alpha)]^2$		

Table 3
Kinetic parameters and correlation coefficient (r) calculated using Coats–Redfern (CR), MacCallum–Tanner (MT) and Horowitz–Metzger (HM) equations

Compound	Model	E_a (kJ mol^{-1})	log A	r	Method
Ia	R1	132.0	12.1	0.99999	CR
	D2	270.2	27.4	0.99997	
	D4	280.8	28.0	0.99992	
	R1	131.9	12.6	0.99999	MT
	D2	270.9	28.2	0.99998	
	D4	281.6	28.8	0.99992	
	R2	155.9	14.7	0.99997	HM
	D2	305.8	30.8	0.99996	
	R1	148.1	13.9	0.99976	
Ib	D2	267.1	29.1	0.99993	CR
	R1	130.5	12.9	0.99990	
	D4	276.1	29.6	0.99971	
	D2	267.3	29.8	0.99993	MT
	R1	129.9	13.4	0.99991	
	D4	276.4	30.2	0.99972	
	D4	298.9	32.2	0.99998	HM
	R1	145.3	14.7	0.99997	
	D2	289.3	31.7	0.99994	
IIa	D2	299.9	33.3	0.99984	CR
	R1	147.22	15.10	0.99978	
	D1	268.1	29.7	0.99967	
	D2	300.4	34.1	0.99985	MT
	R1	146.7	15.6	0.99979	
	D1	268.3	30.4	0.99969	
	D2	316.3	35.3	0.99995	HM
	R1	159.0	16.5	0.99994	
	D4	329.8	36.3	0.99979	

Table 3
(Continued)

Compound	Model	E_a (kJ mol^{-1})	log A	r	Method
IIb	R1	90.4	9.1	0.99995	CR
	D2	186.3	21.5	0.99995	
	D4	193.6	21.8	0.99986	
	R1	88.9	9.5	0.99996	MT
	D2	185.4	22.0	0.99996	
	D4	192.7	22.3	0.99986	
	R2	109.1	11.5	0.99985	HM
	D4	213.9	24.5	0.99981	
	R1	103.6	10.8	0.99957	
IIIa	D2	212.9	21.9	0.99934	CR
	D4	221.2	22.8	0.99931	
	R1	103.3	9.3	0.99928	
	D2	213.0	22.5	0.99939	MT
	R1	102.7	9.8	0.99939	
	D4	221.3	22.9	0.99935	
	R2	124.7	11.7	0.99907	HM
	D4	244.7	25.0	0.99903	
	D3	262.9	27.2	0.99877	
IIIb	D1	206.4	23.0	0.99964	CR
	D2	226.2	25.9	0.99959	
	P3	46.4	3.0	0.99954	
	D1	206.6	23.5	0.99966	MT
	P3	45.0	3.6	0.99966	
	D2	226.2	25.9	0.99961	
	R1	122.8	12.6	0.99988	HM
	D2	244.6	27.6	0.99988	
	D4	253.1	28.0	0.99977	
IVa	D4	203.1	21.2	0.99991	CR
	R1	94.7	8.7	0.99985	
	R2	100.1	9.3	0.99979	
	D4	202.8	21.8	0.99992	MT
	R1	93.7	9.2	0.99988	
	D2	195.0	21.4	0.99984	
	R2	115.3	11.2	0.99974	HM
	D3	242.8	26.1	0.99961	
	R3	121.4	11.8	0.99961	
IVb	D3	240.1	26.3	0.99923	CR
	R3	116.6	11.5	0.99918	
	R2	110.7	10.9	0.99877	

Table 3
(Continued)

Compound	Model	E_a (kJ mol^{-1})	log A	r	Method
	D3	239.9	26.9	0.99928	MT
	R3	115.6	12.0	0.99928	
	R2	109.7	11.4	0.99893	
	F1	145.0	15.6	0.99900	HM
	A3	48.3	3.3	0.99900	
	A4	36.2	1.7	0.99900	
Va	D3	226.2	24.6	0.99771	CR
	R3	109.6	10.6	0.99756	
	R2	103.5	10.0	0.99697	
	D3	225.9	25.2	0.99784	MT
	R3	108.6	11.1	0.99784	
	R2	102.5	10.4	0.99736	
	A2	68.64	5.94	0.99801	HM
	A1.5	91.53	8.86	0.99801	
	A3	45.76	2.97	0.99801	
Vb	D2	106.2	10.9	0.99859	CR
	R1	50.1	3.6	0.99826	
	D1	95.9	9.7	0.99812	
	D2	104.7	11.3	0.99875	MT
	R1	48.3	4.1	0.99863	
	D1	94.4	10.1	0.99840	
	D4	130.8	13.5	0.99824	HM
	R2	66.7	5.8	0.99817	
	R1	63.3	5.4	0.99809	

References

[1] H. le Bozec, D. Touchard and P.H. Dixneuf, in F.G.A. Stone and R. West (Eds.), Advances in Organometallic Chemistry, Vol. 29, Academic Press, London (1989) p. 163.

[2] G. García, I. Solano, G. Sánchez, M.D. Santana, G. López, J. Casabó, E. Molins and C. Miravitlles, J. Organomet. Chem., 467 (1994) 119.

[3] G. García, I. Solano, G. Sánchez, G. López, J. Casabó, E. Molins and C. Miravitlles, Polyhedron, 14 (1995) 1855.

[4] P. Pertici, S. Bertozzi, R. Lazzaroni, G. Vitulli and M.A. Bennett, J. Organomet. Chem., 354 (1988) 117.

[5] G. Sánchez, I. Solano, M.D. Santana, G. García, J. Gálvez and G. López, Thermochim. Acta, 211 (1992) 163.

[6] M.A. Bennett and T.W. Matheson, J. Organomet. Chem., 175 (1979) 87.

[7] R.T. Swann, A.W. Hanson and V. Beokelheide, J. Am. Chem. Soc., 108 (1986) 3324.

[8] M. Gaye, B. Demerseman and P.H. Dixneuf, J. Organomet. Chem., 411 (1991) 263.

[9] R.S. Bates, M.J. Begley and A.H. Wright, Polyhedron, 9 (1990) 113.

[10] A.W. Coats and P.J. Redfern, Nature, 201 (1964) 68.

[11] J.R. MacCallum and J. Tanner, Eur. Polym. J., 6 (1970) 1033.

[12] H.H. Horowitz and G. Metzger, Anal. Chem., 25 (1963) 1964.